

is observed for solutions of alkyllithium reagents in saturated hydrocarbon solvents: G. E. Hartwell and T. L. Brown, *J. Am. Chem. Soc.*, **88**, 4625 (1966).

- (7) This proposal is based on the fact that crystalline tetrakis[iodo(tri-*n*-butylphosphine)copper(I)], which has structure **8** ( $R = I$ ),<sup>8</sup> is also tetrameric in benzene solution.<sup>9</sup>
- (8) A. F. Wells, *Z. Kristallogr., Kristallgeom., Kristallphys., Kristallchem.*, **94**, 447 (1936).

- (9) F. G. Mann, D. Purdie, and A. F. Wells, *J. Chem. Soc.*, 1503 (1936).
- (10) E. C. Ashby and J. J. Watkins, *J. Am. Chem. Soc.*, **99**, 5312 (1977).
- (11) J. San Filippo, Jr., L. E. Zyontz, and J. Potenza, *Inorg. Chem.*, **14**, 1667 (1975), and references therein.
- (12) P. West and R. Waack, *J. Am. Chem. Soc.*, **89**, 4395 (1967).
- (13) (a) T. L. Brown, *Adv. Organomet. Chem.*, **3**, 365 (1965); (b) L. M. Seitz and T. L. Brown, *J. Am. Chem. Soc.*, **88**, 2174 (1966).
- (14) See also ref 10.

Contribution from the Department of Chemistry and the Division of Engineering, Brown University, Providence, Rhode Island 02912

## Crystal Growth and Characterization of the Transition-Metal Phosphides $\text{CuP}_2$ , $\text{NiP}_2$ , and $\text{RhP}_3$

J. P. ODILE, S. SOLED, C. A. CASTRO, and A. WOLD\*

Received June 20, 1977

Single crystals of the transition-metal phosphides  $\text{CuP}_2$ ,  $\text{NiP}_2$ , and  $\text{RhP}_3$  were grown from a tin flux, and, for the first time, their physical properties have been well characterized. In addition, single crystals of  $\text{CuP}_2$  were grown by the chemical-vapor transport technique, using chlorine as a transport agent. All three phosphides crystallize with structures having groups of anions bonded to one another. Although a tin content of 0.6 wt % was measured by atomic absorption in the flux-grown  $\text{CuP}_2$  crystals, the magnetic, electrical, and optical properties of the flux and transported single crystals were very similar. From this study,  $\text{CuP}_2$  was ascertained to be a diamagnetic p-type semiconductor with a band gap of 1.53 eV and  $\text{NiP}_2$  a diamagnetic n-type semiconductor with a band gap of 0.73 eV. p-Type metallic conduction and diamagnetic behavior were observed for  $\text{RhP}_3$ .

### Introduction

Most of the early investigations of transition-metal phosphides have focused on metal-rich phases. The study of the phosphorus-rich transition-metal phosphides has been complicated by the formation of multiple phases during synthesis via direct combination of the elements and by difficulties in crystal growth.<sup>1,2</sup> However, a recent interest in the semiconducting properties of these phases has prompted a more systematic study. Investigators from this laboratory have grown crystals of platinum diphosphide from a tin flux<sup>3</sup> and cobalt triphosphide using the chemical-vapor transport technique.<sup>4</sup> These techniques were used in the present work to prepare single crystals of the phosphorus-rich transition-metal phosphides  $\text{CuP}_2$ ,  $\text{NiP}_2$ , and  $\text{RhP}_3$ .

These phosphides feature different types of anion arrangements. In the  $\text{CuP}_2$  structure, the anion framework is comprised of edge-sharing ten-membered puckered rings of phosphorus atoms lying approximately parallel to (100), that is, in a direction perpendicular to the plane of projection shown in Figure 1. Discrete pairs of copper atoms bridge these rings.

In  $\text{NiP}_2$ , the phosphorus atoms form square rings slightly tilted from the (101) plane as shown in Figure 2 with nickel atoms situated in the center of the rings. Short P-P bonds connect the atoms in adjacent planes.

$\text{RhP}_3$  adopts the skutterudite<sup>5</sup> structure. The phosphorus atoms cluster into planar four-membered rectangular rings, as illustrated in Figure 3. The cations are octahedrally coordinated by the anions whereas each anion is coordinated by two metal atoms and two other anions in a distorted tetrahedron. The unit cell is cubic and contains eight  $\text{RhP}_3$  units.

Large (approximate average dimensions  $2 \times 2 \times 0.5$  mm) and well-characterized single crystals have been grown in order to determine the exact physical properties of these phases.

### Experimental Section

(1) **Chemical Vapor Transport.** Both copper (Johnson-Matthey, 99.999%) and nickel (Gallard-Schlessinger, 99.999%) were reduced in a dry 15%  $\text{H}_2$ /85% Ar atmosphere for 4 h at 600 °C to remove

Table I. Experimental Growth Conditions and Results for the Tin-Flux Method<sup>a</sup>

Nominal compn	Metal/phosphorus/tin molar ratios	Results
$\text{CuP}_2$	1/2/5	Good crystals
$\text{CuP}_2$	1/2/10	Best crystals
$\text{CuP}_2$	1/2/20	Good crystals
$\text{CuP}_3$	1/3/20	Crystals of $\text{Cu}_4\text{SnP}_{10}$
$\text{CuP}_4$	1/4/20	Crystals of $\text{Cu}_4\text{SnP}_{10}$
$\text{CuP}_6$	1/6/20	Crystals of $\text{Cu}_4\text{SnP}_{10}$
$\text{NiP}_2$	1/2/20	Good crystals
$\text{NiP}_2$	1/2/40	Good crystals
$\text{NiP}_3$	1/5/40	Crystals of $\text{NiP}_2$
$\text{RhP}_3$	1/3/40	Best crystals
$\text{RhP}_3$	1/3/80	Good crystals
$\text{RhP}_6$	1/6/10	Crystals of $\text{RhP}_3$

<sup>a</sup> Soaking temperature 1150 °C; cooling rate 5 °C/h; duration 1 week.

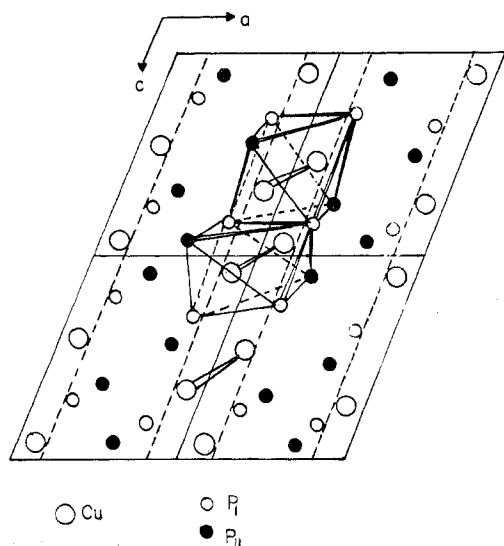
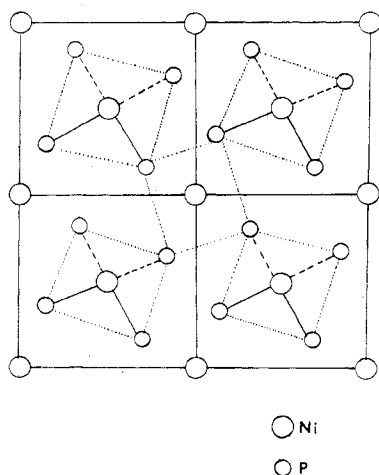
oxygen impurities. Rhodium (Engelhard, 99.99%), red phosphorus (Leico Industries, 99.999%) and chlorine (Linde, 99%) were used as supplied.

In order to prepare single crystals of  $\text{CuP}_2$ , stoichiometric amounts of the starting materials were introduced into silica tubes (28 cm  $\times$  13 mm) which were then evacuated to less than 2 Torr. After the tubes were filled to a pressure of 50 Torr of chlorine, they were sealed and placed in a transport furnace. A temperature profile was maintained for 1 day with the growth zone at 835 °C and the charge zone at 815 °C to remove any potential nucleation sites from the growth zone. After thermal equilibrium was established along the tube, the charge zone was set at 810 °C and the growth zone cooled over a period of 4 days to a final temperature of 760 °C. This gradient was maintained for 3–5 days, and then the furnace was shut down and allowed to cool to room temperature. Large black, shiny crystals of  $\text{CuP}_2$  were obtained by this method. Similar attempts to grow crystals of  $\text{NiP}_2$  and  $\text{RhP}_3$  were unsuccessful.

(2) **Growth from a Tin Flux.** Single crystals of  $\text{CuP}_2$ ,  $\text{NiP}_2$ , and  $\text{RhP}_3$  were grown from a tin flux.<sup>6</sup> The tin metal (99.5%) was purified by melting under a dynamic vacuum. Stoichiometric amounts of the transition metal (Cu, Ni, or Rh) and phosphorus were placed in a silica tube and tin was added such that the resulting mixture was at

Table II. Crystallographic Data and Densities for  $\text{CuP}_2$ ,  $\text{NiP}_2$ , and  $\text{RhP}_3$ 

Compd	Space group	$a_0, \text{\AA}$	$b_0, \text{\AA}$	$c_0, \text{\AA}$	$\beta, \text{deg}$	$d_{\text{calc}}, \text{g/cm}^3$	$d_{\text{obsd}}, \text{g/cm}^3$
$\text{CuP}_2$ (CVT)	$P2_1/c$	5.797	4.803	7.514	112.68	4.32	4.33
$\text{CuP}_2$ (tin flux)	$P2_1/c$	5.796	4.803	7.517	112.66	4.32	4.35
$\text{CuP}_2^9$	$P2_1/c$	5.802	4.807	7.525	112.68		
$\text{NiP}_2$	$C2/c$	6.363	5.615	6.072	126.23	4.57	4.58
$\text{NiP}_2^{10}$	$C2/c$ or $Cc$	6.366	5.615	6.072	126.22		
$\text{RhP}_3$	$Im\bar{3}$	7.991				5.09	5.07
$\text{RhP}_3^{11}$	$Im\bar{3}$	7.9951					

Figure 1.  $\text{CuP}_2$  structure projected on  $(010)$ .Figure 2.  $\text{NiP}_2$  structure projected on  $(10\bar{1})$ .

least 85% tin by weight. The exact molar ratios are listed in Table I. The tube was then evacuated to 2 Torr, sealed, and heated in a furnace at  $35^\circ\text{C/h}$  to  $1150^\circ\text{C}$ . After a soaking period of 12–15 h at this temperature, the furnace was cooled at a constant rate of  $5^\circ\text{C/h}$  to  $550^\circ\text{C}$ . The tube was then removed from the furnace, allowed to cool to room temperature, and opened. Crystals were retrieved by leaching away the solidified flux with hot dilute HCl. The crystals of each phase were black, weighing up to 200 mg. Attempts to grow compositions with a higher phosphorus content resulted in the formation of the already reported phase  $\text{Cu}_4\text{SnP}_{10}$  in the Cu–P system.<sup>7</sup> In the Ni–P and Rh–P systems,  $\text{NiP}_2$  and  $\text{RhP}_3$  were the only phosphorus-rich phases found.

(3) **Chemical Analysis.**  $\text{NiP}_2$  was analyzed for nickel using the photometric dimethylglyoxime method.<sup>8</sup> After 115 mg of crystals were dissolved in boiling aqua regia, the solution was diluted to 250 mL with distilled water. To 1 mL of this solution were added 1 mL of saturated bromine water, 4 mL of concentrated  $\text{NH}_4\text{OH}$ , 35 mL of ethanol, and 20 mL of a solution of dimethylglyoxime and ethanol (0.2 g of DMG in 20 mL of EtOH). The resulting solution was diluted

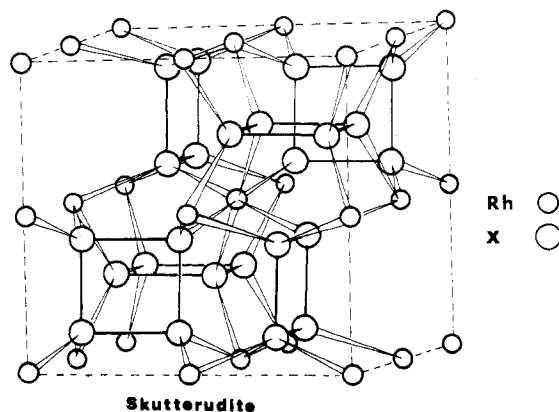


Figure 3. Skutterudite structure.

to 100 mL with distilled water. The absorbance of the brownish nickel–dmg complex was measured at 540 nm using a Cary 14 spectrophotometer. The results were compared with standard nickel solutions made up by dissolving freshly reduced nickel powder in concentrated HCl. The standards obeyed Beer's law in the concentration range 1–3  $\mu\text{g}$  of Ni/mL. From the standard plot, an experimental wt % of nickel of 49 (1%) was calculated and found to be in good agreement with the theoretical value of 48.7% in  $\text{NiP}_2$ .

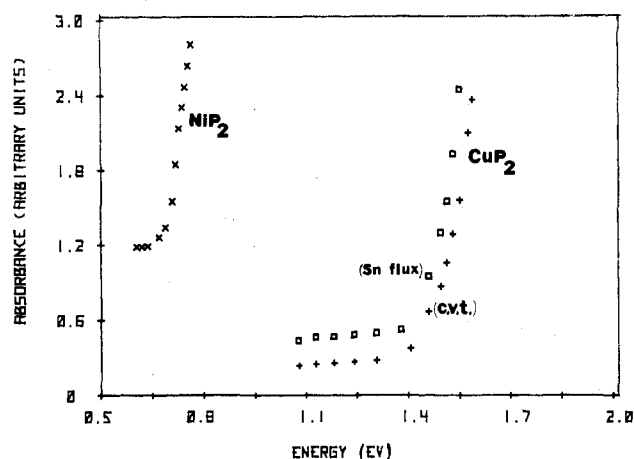
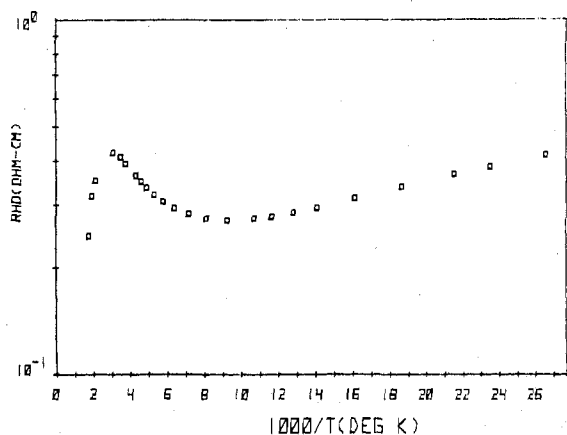
In order to check for flux contamination, single crystals of flux-grown  $\text{CuP}_2$  and  $\text{NiP}_2$  were analyzed for tin content by atomic absorption by Jarrell-Ash (Waltham, Mass.). Weight percents of tin of 0.6% and 1.2% were found for  $\text{CuP}_2$  and  $\text{NiP}_2$ , respectively.

## Results

(1) **X-Ray and Density Measurements.** Powder diffraction patterns of ground single crystals of the different samples were obtained with a Norelco diffractometer using monochromatic radiation from a high-intensity copper source ( $\lambda_{\text{CuK}\alpha_1}$  1.5405  $\text{\AA}$ ). Cell parameters were determined from slow-scan ( $1/4^\circ/\text{min}$ ) diffraction patterns over the range  $12^\circ \leq 2\theta \leq 130^\circ$  with pure powdered silicon (Gallard-Schlesinger, 99.9999%) as an internal standard. The reflections were indexed on unit cells determined from single-crystal studies of previous investigations<sup>9–11</sup> and the precise lattice parameters were obtained using a least-squares refinement from these reflections. The crystallographic data are listed in Table II.

The densities were determined using the hydrostatic technique.<sup>12</sup> Perfluoro(1-methyldecalin) was used as a liquid and its density calibrated before each measurement with a silicon crystal ( $d = 2.328 \text{ g cm}^{-3}$  at  $22^\circ\text{C}$ ). The good agreement between the experimental densities and the densities calculated from the cell parameters confirmed the stoichiometry of the phases.

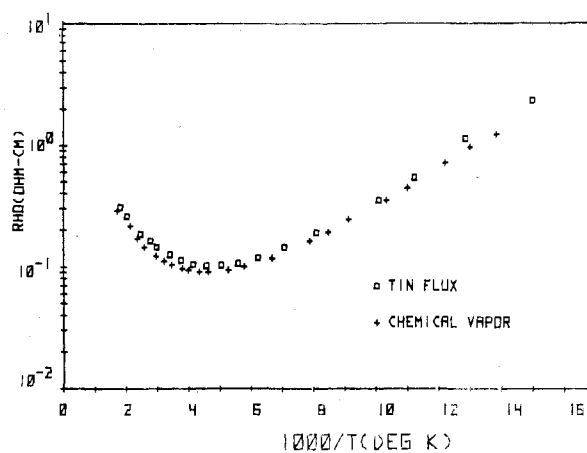
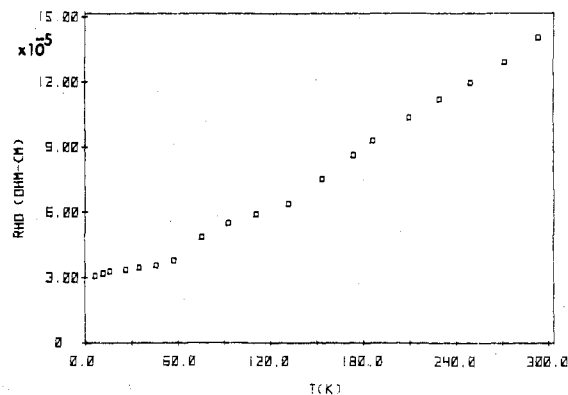
(2) **Magnetic, Optical, and Electrical Measurements.** Magnetic measurements were performed using the Faraday balance previously described by Morris and Wold.<sup>13</sup> The magnetic susceptibilities were measured as a function of temperature from 77 to 300 K at a field strength of 10.3 kOe. The molar susceptibilities of  $\text{CuP}_2$  grown by chemical vapor transport ( $\chi_M = -42.6 \text{ emu}$ ) and of  $\text{CuP}_2$  ( $\chi_M = -44.2 \text{ emu}$ ),  $\text{NiP}_2$  ( $\chi_M = -19.0 \text{ emu}$ ), and  $\text{RhP}_3$  ( $\chi_M = -33.6 \text{ emu}$ ) all grown from a tin flux are negative and temperature independent thus indicating diamagnetic behavior. No corrections

Figure 4. Optical absorption spectrum for  $\text{CuP}_2$  and  $\text{NiP}_2$ .Figure 5. Resistivity vs.  $10^3/T$  for  $\text{NiP}_2$ .

were made for the core diamagnetism of these samples because of the large uncertainty in the magnitude of the corrections compared to the magnitude of the values of the measured susceptibilities. The absence of ferromagnetic impurities in the crystals investigated was ascertained by the lack of field dependence of the susceptibility.

Optical measurements on polished single crystals were performed at room temperature on a Cary 17 dual-beam scanning spectrophotometer operating in the absorbance mode over the range 25000–3500 Å. From these measurements, the values of the optical band gaps were found to be  $E_g = 1.55$  (5) eV for  $\text{CuP}_2$  grown by chemical vapor transport,  $E_g = 1.51$  (5) eV for  $\text{CuP}_2$  grown from a tin flux, and  $E_g = 0.73$  (5) eV for  $\text{NiP}_2$  (Figure 4). An absorption edge was not detected for  $\text{RhP}_3$ , either with the Cary 17 or with the Fourier transform spectrometer scanning at higher wavelengths.

The van der Pauw<sup>14</sup> method was used to measure electrical resistivities and Hall voltages. Room-temperature Seebeck coefficients were measured by applying a thermal gradient to the sample and recording the resulting voltage drop. The room-temperature resistivity of  $\text{NiP}_2$  crystals selected from two different batches prepared in the same manner (as described in the Experimental Section) ranged from 0.42 to 0.09  $\Omega$  cm. Figure 5 shows the electrical resistivity of one of these crystals measured as a function of  $10^3/T$  from 35 to 560 K. The resistivity of  $\text{NiP}_2$  decreases with increasing temperature between 35 and 100 K. This behavior is characteristic of the extrinsic resistivity of a semiconductor at low temperature and is due to the promotion of electrons from impurity levels to the conduction band. The value of the activation energy of the impurity levels calculated from this extrinsic region is 0.002 eV. Between 100 and 320 K, the slope of the resistivity plot

Figure 6. Resistivity vs.  $10^3/T$  for  $\text{CuP}_2$ .Figure 7. Resistivity vs.  $T$  for  $\text{RhP}_3$ .Table III. Room-Temperature Resistivity Values for Different  $\text{CuP}_2$  Samples

Growth technique	$\rho$ , $\Omega$ cm	Growth technique	$\rho$ , $\Omega$ cm
CVT	0.103	Tin flux (1/2/10)	0.126
Tin flux (1/2/5)	0.139	Tin flux (1/2/20)	0.145

changes sign. All the electrons from the impurity levels have been promoted to the conduction band and although the number of carriers remains essentially constant, their mobility decreases because of increased scattering by lattice vibrations, thus causing a rise in the value of the resistivity. Above  $T = 320$  K, the thermal energy promotes an increased number of electrons from the valence to the conduction band. This causes a rapid decrease in the resistivity with increasing temperature and represents the onset of the intrinsic region. From this intrinsic range, a lower bound of 0.3 eV was calculated for the thermal band gap. From Seebeck and Hall measurements, the sign of the majority carriers was found to be negative. The number of majority carriers was calculated assuming a single-band conduction model.

The temperature dependence of the resistivity of a flux-grown crystal of  $\text{CuP}_2$  is compared with the resistivity of a  $\text{CuP}_2$  crystal grown by chemical vapor transport in the temperature range 70–570 K (Figure 6). As seen in this figure, the resistivity plots for both materials are nearly coincident. From the linear segment of each plot (70–220 K), the activation energy of impurity states in the extrinsic region was calculated to be 0.03 eV for both samples. The exhaustion region occurs above 220 K for these samples. Contrary to the  $\text{NiP}_2$  case, the onset of the intrinsic region could not be reached in the temperature range studied. This reflects the fact that the band gap of  $\text{CuP}_2$  is approximately twice that of  $\text{NiP}_2$ . The room-temperature resistivity values for four different  $\text{CuP}_2$

Table IV. Transport Properties of  $\text{CuP}_2$ ,  $\text{NiP}_2$ , and  $\text{RhP}_3$ 

	$\text{CuP}_2$ (chemical vapor)	$\text{CuP}_2$ (tin flux)	$\text{NiP}_2$	$\text{RhP}_3$
$\rho_{77\text{K}}$ , $\Omega$ cm	0.97	1.14	0.29	$4.87 \times 10^{-5}$
$\rho_{290\text{K}}$ , $\Omega$ cm	0.106	0.126	0.39	$14.03 \times 10^{-5}$
No. of carriers (77 K)	$1.0 \times 10^{16}$	$0.6 \times 10^{16}$	$7.3 \times 10^{17}$	$0.37 \times 10^{20}$
No. of carriers (290 K)	$6.6 \times 10^{17}$	$4.3 \times 10^{17}$	$8.7 \times 10^{17}$	$0.6 \times 10^{20}$
Sign of carriers				
Hall	+	+	-	+
Seebeck	+	+	-	+
Seebeck coeff, $\mu\text{V}/^\circ\text{C}$		692	392	32
Activation en- ergy of impu- rity levels, eV	0.03	0.03	0.002	
Optical absorp- tion edge, eV	1.55	1.51	0.73	

samples are listed in Table III. p-Type conduction was determined from Seebeck and Hall measurements.

Figure 7 shows that the resistivity of  $\text{RhP}_3$  increases with increasing temperature over the whole temperature range studied (4–300 K).

### Conclusion

From this study of single crystals grown from a tin flux,  $\text{NiP}_2$  was ascertained to be a diamagnetic n-type semiconductor with a band gap of 0.7 eV. The observed diamagnetic behavior of  $\text{NiP}_2$  is consistent with the presence of low-spin  $d^8$  configuration for the nickel atom.

The magnetic, optical, and electrical properties of single crystals of  $\text{CuP}_2$  grown from a tin flux were studied and found to be very similar to those of single crystals of  $\text{CuP}_2$  grown

by the chemical-vapor transport technique. This similarity indicates that the tin did not substitute chemically into the  $\text{CuP}_2$  structure but rather occurred as inclusions, as observed experimentally on flux-grown crystals.

The negative and temperature-independent magnetic susceptibility of  $\text{RhP}_3$  indicates the presence of low-spin state  $d^6$  rhodium in this compound. Hall, Seebeck, and resistivity measurements indicate p-type metallic conduction.

Table IV summarizes the transport properties of the different phases investigated.

**Acknowledgment.** This work was supported by the U.S. Army Research Office, Triangle Park, N.C., the Materials Research Laboratory Program at Brown University, and the National Science Foundation (Grant No. GF 39737).

**Registry No.**  $\text{CuP}_2$ , 12019-11-3;  $\text{NiP}_2$ , 12035-47-1;  $\text{RhP}_3$ , 12202-48-1.

### References and Notes

- (1) W. Blitz and M. Heimbrecht, *Z. Anorg. Allg. Chem.*, **237**, 132 (1938).
- (2) A. Wilson, in "Mellor's Comprehensive Treatise on Inorganic and Theoretical Chemistry", Vol. 8, Supplement 3, Longmans Green and Co., London, 1922.
- (3) A. Finley, D. Schleich, J. Ackermann, S. Soled, and A. Wold, *Mater. Res. Bull.*, **9**, 1655 (1974).
- (4) J. Ackermann and A. Wold, *J. Phys. Chem. Solids*, in press.
- (5) I. Oftedal, *Z. Kristallogr., Kristallgeom., Kristallphys., Kristallchem.*, **66**, 517 (1928).
- (6) D. Elwell and H. J. Scheel, "Crystal Growth from High Temperature Solutions", Academic Press, London, 1975.
- (7) N. A. Goryunova, V. M. Orlov, V. I. Sokolova, G. P. Shpenkov, and E. V. Tsvetkova, *Phys. Status Solidi*, **3**, 75 (1970).
- (8) E. B. Sandell, "Colorimetric Determination of Traces of Metals", Vol. III, 2nd ed, Interscience, New York, N.Y. 1950, p 470.
- (9) O. Olofsson, *Acta Chem. Scand.*, **19**, 229 (1965).
- (10) E. Larsson, *Ark. Kemi*, **23**, 335 (1964).
- (11) S. Rundqvist and N. O. Ersson, *Ark. Kemi*, **30**, 103 (1968).
- (12) R. L. Adams, Ph.D. Thesis, Brown University, 1973.
- (13) B. Morris and A. Wold, *Rev. Sci. Instrum.*, **39**, 1937 (1968).
- (14) L. J. van der Pauw, *Philips Res. Rep.*, **13**, 1 (1958).

Contribution from the Departments of Chemistry, University of Missouri at Kansas City, Kansas City, Missouri 64110, and University of South Carolina, Columbia, South Carolina 29208.

## An Infrared and Raman Study of 1,2-Dimethyldiphosphine

JAMES R. BARD,<sup>1a,b</sup> ANTONIO A. SANDOVAL,<sup>\*1b</sup> CHARLES J. WURREY,<sup>1b</sup> and JAMES R. DURIG<sup>\*1c</sup>

Received August 9, 1977

The Raman spectra of 1,2-dimethyldiphosphine have been recorded in the liquid and solid phases to  $4000\text{ cm}^{-1}$ . The infrared spectrum of the solid phase was also recorded from  $4000$  to  $200\text{ cm}^{-1}$ . The spectra were consistent with the presence of both the trans and gauche meso conformers and presumably the gauche conformer of the *d,l* isomer in the liquid phase. The gauche meso conformer was absent from the solid phase. A tentative vibrational assignment is proposed for the molecule.

### Introduction

The synthesis, reactions, and structure of diphosphine and certain of its tetrasubstituted derivatives have been the subject of continuing investigations in our laboratories.<sup>2-9</sup> Although there are a number of additional recent theoretical and experimental conformational studies on these types of compounds,<sup>10-17</sup> there are few such reported studies of the 1,2-disubstituted diphosphines.<sup>18,19</sup> No vibrational study has been reported for any 1,2-disubstituted diphosphine although the infrared spectrum of gaseous 1,2-bis(trifluoromethyl)diphosphine has been reported and fragmentary assignments were made.<sup>20</sup> However, no structural conclusions regarding conformers were made from the data.

The successful preparation of diphosphorus tetrachloride by electric discharge in mixtures of phosphorus trichloride and hydrogen<sup>21</sup> has stimulated the recent synthesis of 1,2-dimethyldiphosphine by low-pressure silent electric discharge.<sup>22</sup>

For this molecule, which can exist in both the meso and *d,l* diastereomers, there are a number of possible conformers, which previous studies have shown may be most readily investigated by a study of its vibrational spectra.<sup>4,6</sup> These conformers exist in both the trans and gauche forms, and illustrations representative of each form for similarly substituted diphosphines may be found in the literature.<sup>13,18,19</sup> In this paper, we present results obtained from the infrared and Raman spectra on the structure of 1,2-dimethyldiphosphine.

### Experimental Section

1,2-Dimethyldiphosphine was prepared by passing methylphosphine through a silent electric discharge using a Siemens-type discharge tube.<sup>22</sup> The methylphosphine was prepared by the reduction of dimethyl methylphosphonate with  $\text{LiAlH}_4$  in monoglyme.<sup>23</sup> All sample preparations and manipulations were carried out using standard high-vacuum techniques due to the toxicity of these compounds in general, their ease of oxidation, and the thermal instability of 1,2-dimethyldiphosphine. This compound decomposes rapidly at room